InSAR data as a field guide for mapping minor earthquake surface ruptures: Ground displacements along the Paganica Fault during the 6 April 2009 L'Aquila earthquake

L. Guerrieri,[1] G. Baer,[2] Y. Hamiel,[2] R. Amit,[2] A. M. Blumetti,[1] V. Comerci,[1] P. Di Manna,[1] A. M. Michetti,[3] A. Salamon,[2] A. Mushkin,[2] G. Sileo,[3] and E. Vittori[1]

Received 22 March 2010; revised 2 September 2010; accepted 23 September 2010; published 30 December 2010.

[1] On 6 April 2009, a moderate earthquake (M_w = 6.3; M_l = 5.8) struck the Abruzzo region in central Italy, causing more than 300 fatalities and heavy damage to L'Aquila and surrounding villages. Coseismic surface effects have been thoroughly documented by timely field surveys as well as by remote sensing analyses of satellite images. The outstanding quality of geological, seismological, geodetic, and interferometric synthetic aperture radar (InSAR) information arguably represents the best ever data set made available immediately after a moderate seismic event. Based on this data set, we aim at testing the capability of coupled geological and InSAR data to map surface faulting patterns associated with moderate earthquakes. Coseismic ground ruptures have been mapped at a scale of 1:500 in the whole epicentral area. Traces of surface ruptures have been inferred from linear phase discontinuities identified in the interferogram. A very good agreement between the two methods resulted in the characterization of the main surface rupture along the Paganica fault. The same approach applied to ground ruptures hypothesized along other capable fault segments provided more questionable results. Thus, the combined field and InSAR approach appeared useful for detecting continuous surface ruptures exceeding 1 km in length and showing displacements greater than a few centimeters. These are the typical faulting parameters for moderate earthquakes ($6.0 < M_w < 6.5$) in central Apennines. For continuous ground cracks shorter than a few hundred meters and/or that show displacements smaller than 1–2 cm, the described approach may be less helpful, most probably due to the limited resolution of the data.

Citation: Guerrieri, L., et al. (2010), InSAR data as a field guide for mapping minor earthquake surface ruptures: Ground displacements along the Paganica Fault during the 6 April 2009 L'Aquila earthquake, *J. Geophys. Res.*, *115*, B12331, doi:10.1029/2010JB007579.

1. Introduction

[2] The use of interferometric synthetic aperture radar (InSAR) maps as a guide to field work, particularly for moderate earthquakes and small-scale fault ruptures has been explored only in a very limited number of cases [e.g., *Price and Sandwell*, 1998; *Baer et al.*, 2008]. This paper aims at testing the effective capability of a coupled geological (based on immediate and accurate postseismic field mapping) and InSAR studies to detect and analyze surface faulting associated with moderate seismic events such as the 6 April 2009 M_w 6.3 L'Aquila earthquake [e.g., *Chiarabba et al.*, 2009; *Walters et al.*, 2009; *Wilkinson et al.*, 2010].

[3] To this end, a joint team composed by the Geological Surveys of Italy and Israel and the University of Insubria conducted specific field surveys and precise InSAR analysis of the epicentral area. Clearly, in this case the field survey preceded the InSAR measurements due to the immediately available epicentral location and the good accessibility of the area that allowed surveying the territory already in the first hours after the event, long before the first postearthquake radar satellite images were acquired. Nevertheless, the sensitivity of InSAR to displacements in the satellite to ground line of sight (LOS) is such that even very minor surface ruptures show up in the general deformation fringe pattern, confirming (or not) suspected fault reactivations and contributing to the better understanding of the coseismic events.

[4] Moderate magnitude normal faulting earthquakes associated with small surface fault displacement are typical seismic events in the extensional tectonic setting of the Apennines in Italy [e.g., *Michetti et al.*, 2000]. The L'Aquila

[1]Geological Survey of Italy, High Institute for the Environmental Protection and Research, Rome, Italy.
[2]Geological Survey of Israel, Jerusalem, Israel.
[3]Dipartimento di Scienze Chimiche ed Ambientali, Facoltà di Scienze Matematiche, Fisiche e Naturali, Università degli Studi dell'Insubria, Como, Italy.

0148-0227/10/2010JB007579

event (M_l 5.8, M_w 6.3, hypocentral depth 9 km) occurred on 6 April 2009 at 0132 GMT: the epicenter was located very near the historical downtown of L'Aquila (Figure 1), which was severely damaged together with many villages in the surroundings. The death toll was of more than 300 casualties. Two M > 5.0 shocks followed on 7 April (M_l = 5.3; epicenter not far from Fossa, about 10 km southeast of L'Aquila) and on 9 April (M_l = 5.1; epicenter near Campotosto, about 15 km northwest of L'Aquila).

[5] The seismic sequence lasted for several months with M > 4 events even in October 2009, affecting a ~40 km long NW trending zone mostly coinciding with the Middle Aterno River Valley [*Chiarabba et al.*, 2009]. The focal plane solutions clearly define NW trending normal source mechanisms, in good agreement with the tectonic setting of the region, characterized by tectonic valleys and mountain chains bounded by NW trending capable normal faults [e.g., *Blumetti and Guerrieri*, 2007]. The focal depths are generally within 10–12 km, but the 7 April event was slightly anomalous in terms of focal depth (about 15 km) and focal mechanism (having a significant strike-slip component). While most of the main events appear to have occurred on SW dipping planes, the few aftershocks referable to the 7 April event do not yet define a preferred nodal plane for the rupture, leaving for the moment a question mark on its source.

[6] The scenario of damages to buildings compiled by the Quick Earthquake Survey Team (QUEST) [*Galli et al.*, 2009] shows a maximum intensity of IX MCS with a preferred propagation toward southeast from the epicenter and a very irregular pattern. This depends basically on the evolving building practices from masonry to concrete frame (most constructions postdate the XVII century, after the destructive 2 February 1703 earthquake, I° = X MCS) and the local geology, dominated by a valley floor filled by Quaternary lacustrine and alluvial deposits, and steep mountain slopes. In particular, the highest macroseismic intensity values (Intensity ≥ IX MCS) have occurred in isolated localities within areas characterized by a lower level of damages (Intensity ≤ VIII MCS). These peaks of intensity appear to have been caused by a peculiar seismic vulnerability, associated in some cases with evident site effects (e.g., Onna and other villages located on the soft alluvial and lake sediments of the Middle Aterno River Valley).

[7] Several teams of geologists began surveys in the hit area on the very day of the main shock, looking for evidence of seismogenic environmental effects, especially surface rupturing whose first hint was given by the rupture of the Gran Sasso Aqueduct across the Paganica Fault (see the Geological Sheet "L'Aquila" [*Servizio Geologico d'Italia*, 2006]). Immediate investigations along this fault identified clear evidence of reactivation, in the form of ground cracks, sometimes displaying a modest vertical offset, only occasionally exceeding 8–10 cm, aligned almost continuously in a narrow belt at least 2.6 km long. The estimate of the total surface rupture length ranges from about 3 to 19 km according to different authors [*Blumetti et al.*, 2009; *Emergeo Working Group*, 2010; *Falcucci et al.*, 2009; *Galli et al.*, 2009; *Roberts et al.*, 2010; E. Vittori et al., Surface faulting of the April 6, 2009, *Mw* 6.3 L'Aquila earthquake in central Italy, submitted to *Bulletin of the Seismological Society of America*, 2010]. Other authors interpreted the observed ground cracks as secondary phenomena indirectly connected to the causative earthquake source fault at depth [e.g., *Valensise*, 2009]. This uncertainty in the actual dimensions and geometry of the tectonic surface ruptures was one of the main motivations for our study.

[8] Synthetic aperture radar (SAR) data were distributed by the European Space Agency (ESA) a few days after the main shock. Published InSAR results revealed with increasing clarity the amount and extent of the deformation and confirmed the location of the main fault rupture and the area of maximal subsidence [*Atzori et al.*, 2009; *Walters et al.*, 2009]. While most of the published models agree with the general pattern of deformation, they provided ambiguous results regarding the upward extension of the surface slip along the fault. This is typical for moderate earthquakes (M_w around 6) particularly when surface deformation and displacements are too small for unequivocal source parameter inversion [e.g., *Vittori et al.*, 2000; *Salvi et al.*, 2000; *Biggs et al.*, 2006].

[9] In the following, we compare detailed field measurements of coseismic ground displacement and InSAR maps in order to test the resolution of InSAR observations for understanding primary surface rupture processes during moderate magnitude earthquakes. The L'Aquila seismic event provides in fact a unique data set for this test, due to the outstanding quality of geological, seismological, geodetic,

Figure 1. Seismotectonic framework of the study area with location of surface effects along capable faults. The 2009 L'Aquila seismic sequence was characterized by three main shocks (red and orange stars with corresponding focal mechanism). A yellow dashed line delimits the area with aftershocks occurred in the period 6 April to 20 July (source is INGV). Smaller yellow stars locate the epicenters of relevant historical earthquakes (source is CPTI08). Red lines locate capable faults (source is ITHACA database, www.apat.gov.it/site/en-GB/Projects/ITHACA_-_ITaly_HAzards_from_CApable_faults/default.html) named by the following acronyms (in blue): ASG, Assergi fault; BAR, Barisciano fault; BAZ, Bazzano fault; CAP, Capitignano fault; CAT, Colle Caticchio fault; CCE, Colle Cerasitto fault; CEN, Colle Enzano fault; CFE, Campo Felice fault; CIM, Campo Imperatore fault; COF, Colle Frolla fault; COP, Colle Praticciolo fault; LAM, Laga Mountains fault; MAR, Monte D'Aragno fault; MAV, Middle Aterno Valley fault system; MCS, Monte Castellano fault; MDU, Monti della Duchessa fault; MFS, Monticchio-Fossa-Stiffe fault system; MMA, Monte Macchione fault; MOR, Monte Orsello fault; MRZ, Monte Ruzza fault; MSF, Monte San Franco fault; OPP, Ovindoli-Piani di Pezza fault; PAG, Paganica fault; PET, Monte Pettino fault; PIZ, Pizzoli fault; ROC, Roio-Canetre fault; SDE, San Demetrio faults system; SCI, Scindarella fault; SMA, San Martino fault; SSS, Santo Stefano di Sessanio fault system; STB, Stabiata fault; TRS, Tre Selle fault; VAS, Valle degli Asini fault; VEM, Velino-Magnola fault; VDS, Valle del Salto fault. Coseismic geological effects along capable faults that are described in Table 2 (except the Paganica Fault mapped in Figure 3) are indicated by dots colored according to the measured maximum field offset (see legend at the top right). White labels report the corresponding numbers in Table 2. The A-B purple line shows the trace of the geological cross section (Figure 2). Blue dashed box in the Paganica area locates Figure 3.

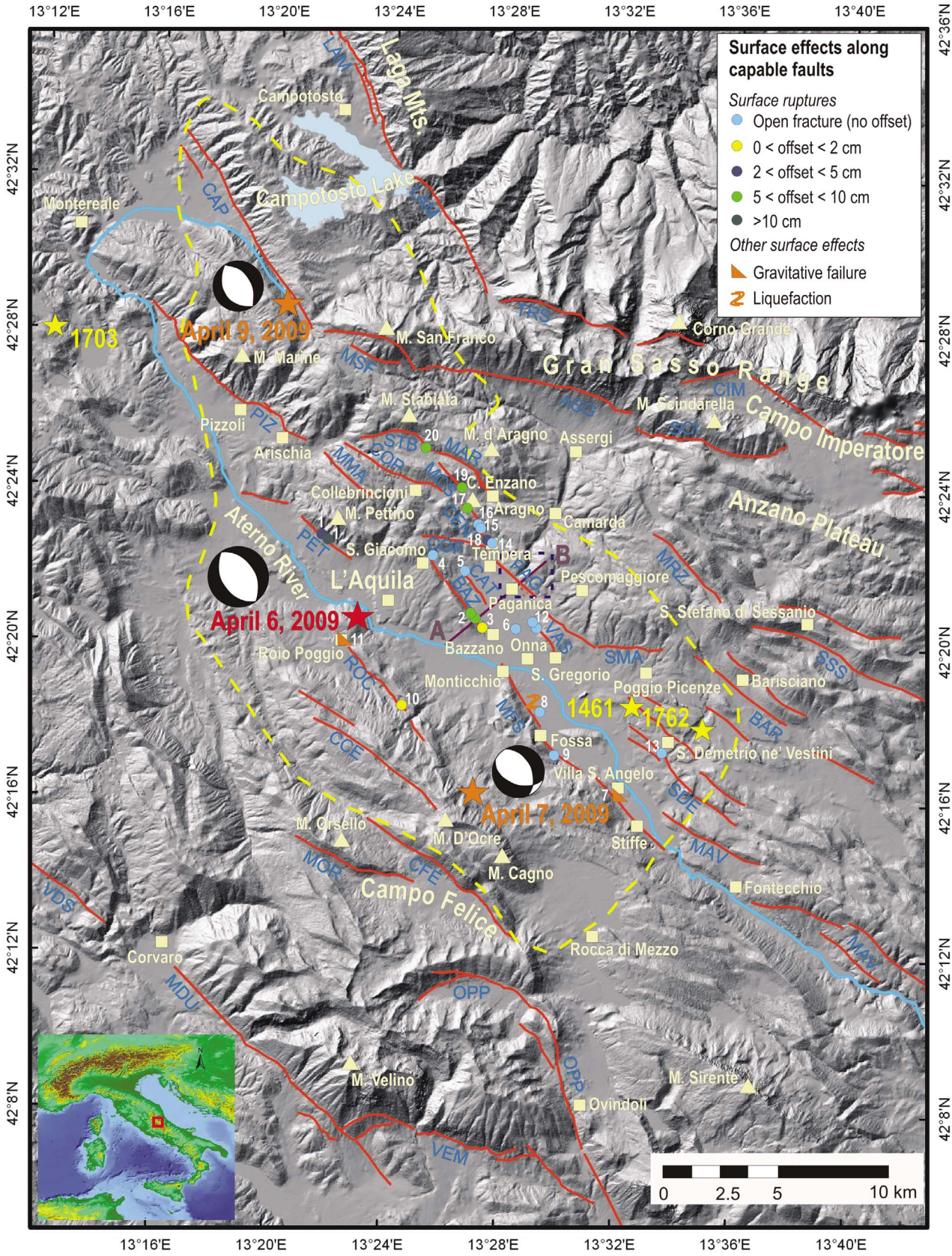
Surface effects along capable faults
Surface ruptures
Open fracture (no offset)
0 < offset < 2 cm
2 < offset < 5 cm
5 < offset < 10 cm
>10 cm
Other surface effects
Gravitative failure
Liquefaction
13°12'E
13°16'E
13°20'E
13°24'E
13°28'E
13°32'E
13°36'E
13°40'E
42°36'N
42°32'N
42°28'N
42°24'N
42°20'N
42°16'N
42°12'N
42°8'N
Campotosto
Laga Mts.
Campotosto Lake
Montereale
1703
April 9, 2009
M. Marine
M. San Franco
Corno Grande
Gran Sasso Range
M. Scindarella
Campo Imperatore
Anzano Plateau
M. Stabiata
M. d'Aragno
Assergi
Pizzoli
Arischia
Collebrincioni
M. Pettino
C. Enzano
Aragno
Camarda
Aterno River
L'Aquila
S. Giacomo
Tempera
Pescomaggiore
April 6, 2009
Paganica
S. Stefano di Sessanio
Roio Poggio
Bazzano
Onna
S. Gregorio
Monticchio
Poggio Picenze
Barisciano
1461
1762
Fossa
S. Demetrio ne' Vestini
Villa S. Angelo
April 7, 2009
M. Orsello
M. D'Ocre
Stiffe
M. Cagno
Campo Felice
Fontecchio
Rocca di Mezzo
Corvaro
M. Velino
M. Sirente
Ovindoli
0
2.5
5
10 km

Figure 1

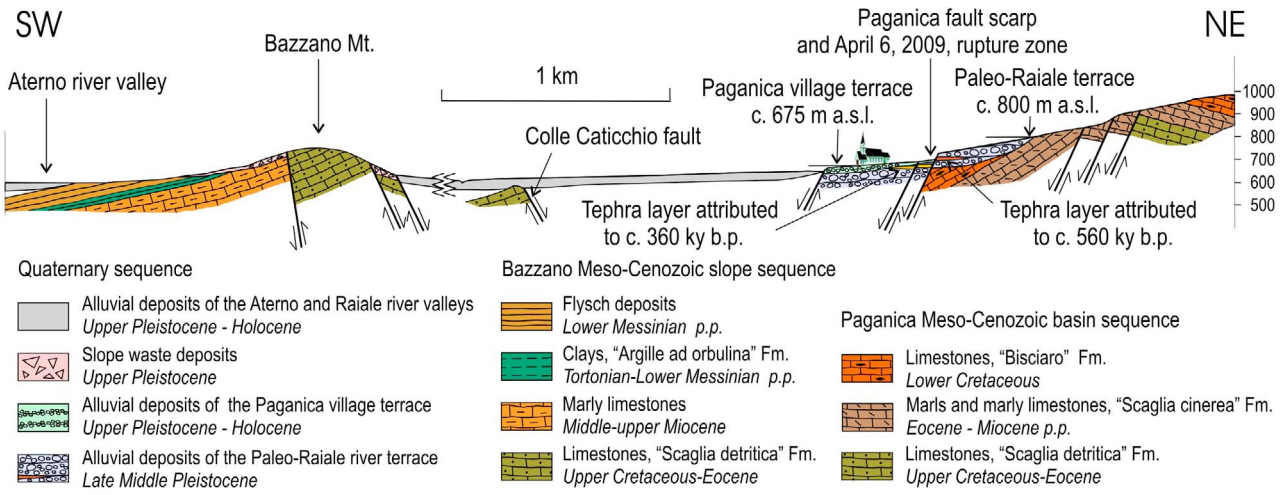

Figure 2. Geological cross section across the Bazzano, Colle Caticchio, and Paganica faults. Trace in Figure 1.

and remote sensing (in particular InSAR) information, made available immediately after the main shock.

2. Seismotectonic Setting of the L'Aquila Area

2.1. Geological Framework

[10] The epicentral area of the 2009 L'Aquila seismic sequence is characterized by a system of NW-SE trending tectonic depressions, located between the Gran Sasso and the Monti d'Ocre morphotectonic units. The outcropping geological formations and the geophysical data reveal a complex structural setting given by several overthrusted tectonic units belonging to the transitional domain between the Latium-Abruzzi carbonate shelf platform and the Umbria-Marche pelagic basin [*Vezzani and Ghisetti*, 1998; *Servizio Geologico d'Italia*, 2006].

[11] Basically, the present structure of the region is the result of Messinian to lower Pliocene orogenic thrust tectonics [*Patacca et al.*, 1992] followed by extension which started at least 2 Ma ago, causing the formation of lacustrine basins developed in a low-relief landscape [*Demangeot*, 1965] and containing mammal fauna (see *Mammuthus* (*Archidiskodon*) *meridionalis vestinus*, Lower Pleistocene [*Maccagno*, 1962; *Azzaroli*, 1977]).

[12] The typical block-faulted morphostructural setting characterized by tectonically controlled basins and ranges [*Serva et al.*, 2002; *Blumetti et al.*, 2004; *Blumetti and Guerrieri*, 2007] is the cumulative effect of this extensional activity at least since the end of the Lower Pleistocene (about 0.8 Ma) when most of the Apennines relief was formed [*Demangeot*, 1965].

[13] Active extensional tectonics is accommodated by a dense array of normal faults (Figure 1). Major tectonic elements are typically located at the base of fault generated mountain fronts, tens of kilometers long and some hundreds of meters high. Subordinate faults within the major blocks determine additional topographic irregularities. During moderate to strong earthquakes (M > 6) all these faults might be rejuvenated up to the surface. Therefore, their total throw is the result of a number of surface faulting events. Crustal extension is still ongoing in this area, as demonstrated by geodetic data [e.g., *D'Agostino et al.*, 2008], seismicity, and paleoseismicity [*Bagnaia et al.*, 1992; *Blumetti*, 1995; *Galadini and Galli*, 2000; *Moro et al.*, 2002; *Papanikolaou et al.*, 2005].

[14] In the northern sector of the 2009 L'Aquila seismic sequence, the Pizzoli and Pettino faults have downthrown the "Upper Aterno Valley" unit from the Monte Marine plateau by at least 700 m in the last 0.8 Ma.

[15] In the southern area, the Paganica–San Demetrio fault [*Bagnaia et al.*, 1992] is located at the boundary between the "Middle Aterno Valley" and the "Gran Sasso" structural units. This latter block which coincides with the highest elevations in the Apennines, is dissected by a set of WNW-ESE trending normal faults including the Assergi and Campo Imperatore faults from 2914 m (Monte Corno Grande) down to about 1500 m at the Anzano Plateau. These faults have a listric geometry showing normal reactivation of old thrusts at depth [*D'Agostino et al.*, 2001], and are cut by the Paganica–San Demetrio high-angle normal fault, which downthrows the Middle Aterno valley region, at an elevation of about 600 m.

[16] At the SW border of the Middle Aterno valley, the Bazzano and Monticchio-Fossa-Stiffe antithetic faults bound the Monti d'Ocre structural unit to the north (Figure 2). Minor faults with en echelon pattern cross this unit (Roio-Canetre, Colle Cerasitto, Campo Felice and Monte Orsello faults). To the south, together with the Piano di Pezza fault, these faults are linked to the Fucino basin fault zone, active during the 13 January 1915 Avezzano earthquake ($M = 7.0$; $I_0 = XI$ MCS [e.g., *Michetti et al.*, 1996]).

[17] Major faults (e.g., high-angle faults with large morphostructural throw) are also those with higher seismogenic potential, capable of producing surface faulting. Capable faults located in the epicentral area are shown in Figure 1 (from Italian Hazard from Capable faults database (ITHACA), according to the state of knowledge on seismotectonic and paleoseismic research). It is important to outline that most of the Quaternary tectonic deformation was accommodated along these faults.

[18] With specific regard to the Paganica fault area, an associated fault generated mountain front is not evident due to the presence of an ancient drainage system at the footwall, which was active since at least the end of the Lower Pleistocene ("Paleo-Raiale" river [*Messina et al.*, 2009]). Relict forms of this ancient landscape as well as different orders of fluvial deposits terraced by the progressive activity of the Paganica fault are still preserved in the footwall (Figure 2). Among them, deposits at about 150 m above the local base level contain tephra layers referred to the eruptions from the Latium volcanic districts which occurred between 560 and 360 ka. These data constrain the Paganica fault long-term slip rate to the order of 0.4 mm/yr.

2.2. Historical Seismicity

[19] In the historical past, several moderate to strong earthquakes affected the epicentral area (Figure 1, source, CPTI08). Two events with Intensity X MCS, but with different estimated magnitudes, occurred on 26 November 1461 and 2 February 1703. Two other destructive earthquakes hit the same area on 9 September 1349, IX-X MCS (epicenter in Valle del Salto, about 20 km SW of L'Aquila) and on 6 October 1762, IX MCS. The strongest and best documented earthquake sequence, occurred in 1703, and was characterized by three main shocks that moved in a few days from NNW to SSE. The third shock, on 2 February (Intensity X MCS), which destroyed the city of L'Aquila causing 2500 casualties [*Baratta*, 1901] (CPTI08), produced surface faulting along the Pizzoli fault for a length of about 20 km [*Blumetti*, 1995; *Moro et al.*, 2002]. Impressive secondary effects were induced by that event, among which there was a huge deep-seated gravitational slide on the Mt. Marine ridge, a large slope movement at Villa Camponeschi, near Posta, several rockfalls, and liquefaction phenomena along the Aterno River [*Parozzani*, 1887; *Uria de Llanos*, 1703]. The 1461 and 1762 events were probably smaller and similar to the 2009 earthquake, both in their magnitudes and epicenter location southeast of L'Aquila, suggesting a return period of ~3 centuries for this type of events.

3. Surface Faulting Along the Paganica Fault

[20] Descriptions of geological effects reported along the Paganica Fault are from *Blumetti et al.* [2009], integrated in some cases with observations published by *Boncio et al.* [2010], *Emergeo Working Group* [2010], *Falcucci et al.* [2009], *Galli et al.* [2009], *Messina et al.* [2009], *Wilkinson et al.* [2010] and Vittori et al. (submitted manuscript, 2010).

3.1. Field Evidence

[21] The most prominent coseismic feature is a set of irregular but very well aligned ruptures, trending 120°N to 140°N along the Paganica fault zone, at the NE margin of the Paganica village. More precisely, the ruptures appear in the hanging wall, at a distance ranging from a few meters to a few tens of meters away from the known main fault scarp (Figure 3). The ruptures were mapped from NW of Tempera (Capo Vera springs) to the Paganica-Pescomaggiore Road at the SE, and affected the natural ground as well as artificial surfaces (paved/concrete roads, parking lots, private gardens) and buildings (floors, walls and concrete frames). In general, the deformation appears along a single major fracture, but in some cases it is also distributed within a rupture zone a few tens of meters wide. In the SE sector, some aligned cracks have allowed to identify a secondary lineament parallel to the main rupture, some hundreds of meters long with no appreciable offset. The cracks caused significant damages to several buildings and infrastructures, including the rupture of the Gran Sasso aqueduct (diameter about 70 cm).

[22] The fault ruptures have been mapped almost continuously for a measured length of 2.6 km. It is noteworthy that many fractures did not display appreciable vertical offsets while others showed throws higher than 10 cm. Considering the postseismic offset of about 2–3 cm within the first days after the main shock [e.g., *McCaffrey et al.*, 2009], the maximum coseismic vertical offset can be evaluated in the order of 7–8 cm.

[23] The ruptures along the Paganica fault have been described also by other authors: according to *Emergeo Working Group* [2010] the coseismic ruptures have been continuous for 2.5 km. Considering also other discontinuous and sporadic breaks mapped to the northwest and to the southeast, the total surface rupture length exceeds 6 km. *Falcucci et al.* [2009] distinguish between a central segment of the fault characterized by uninterrupted coseismic ground cracks (vertical and horizontal offset up to 15 cm), and northern and southern segments (Enzano and Valle degli Asini faults, respectively), along which only discontinuous ruptures without vertical offset have been surveyed.

[24] *Galli et al.* [2009] however, estimate the length of the surface rupture to be in the order of 19 km: besides the main rupture expression between Collebrincioni and San Gregorio, they consider other effects (cracks) located north of Collebrincioni and at San Demetrio ne' Vestini, as evidence of surface faulting.

3.2. InSAR Measurements and Results

[25] InSAR is used here to measure the surface displacements associated with the earthquake (see *Massonnet and Feigl* [1998, and references therein] for details and applications of the technique). We processed advanced synthetic aperture radar images from the European Space Agency (ESA) ENVISAT satellite (C band, 5.6 cm wavelength, I2 beam mode, mean incidence angles of 23°), using the JPL/Caltech ROI-PAC software [*Rosen et al.*, 2004]. Interferograms were made from three image pairs, of ascending (NNW heading) and descending (SSW heading) satellite tracks, that captured the surface deformation associated with the L'Aquila earthquake (Figures 4 and 5a). The interferograms were generated at full (one-look) resolution of 20 m × 20 m pixels using a 20 m pixel Digital Elevation Model (DEM) made for geocoding and removal of the topographic phase (for comparison with four-look resolution, see Figure S1).[1] We reduce the interferometric phase noise and unwrapping residues by applying an adaptive filter based on the local fringe pattern [*Goldstein and Werner*, 1998] with SNR threshold of 0.1. The phase is unwrapped using the branch-cut algorithm [*Goldstein et al.*, 1988]. The deformation field is shown in the forms of a wrapped interferogram, where each fringe cycle corresponds to 28 mm of

[1] Auxiliary materials are available in the HTML. doi:10.1029/2010JB007579.

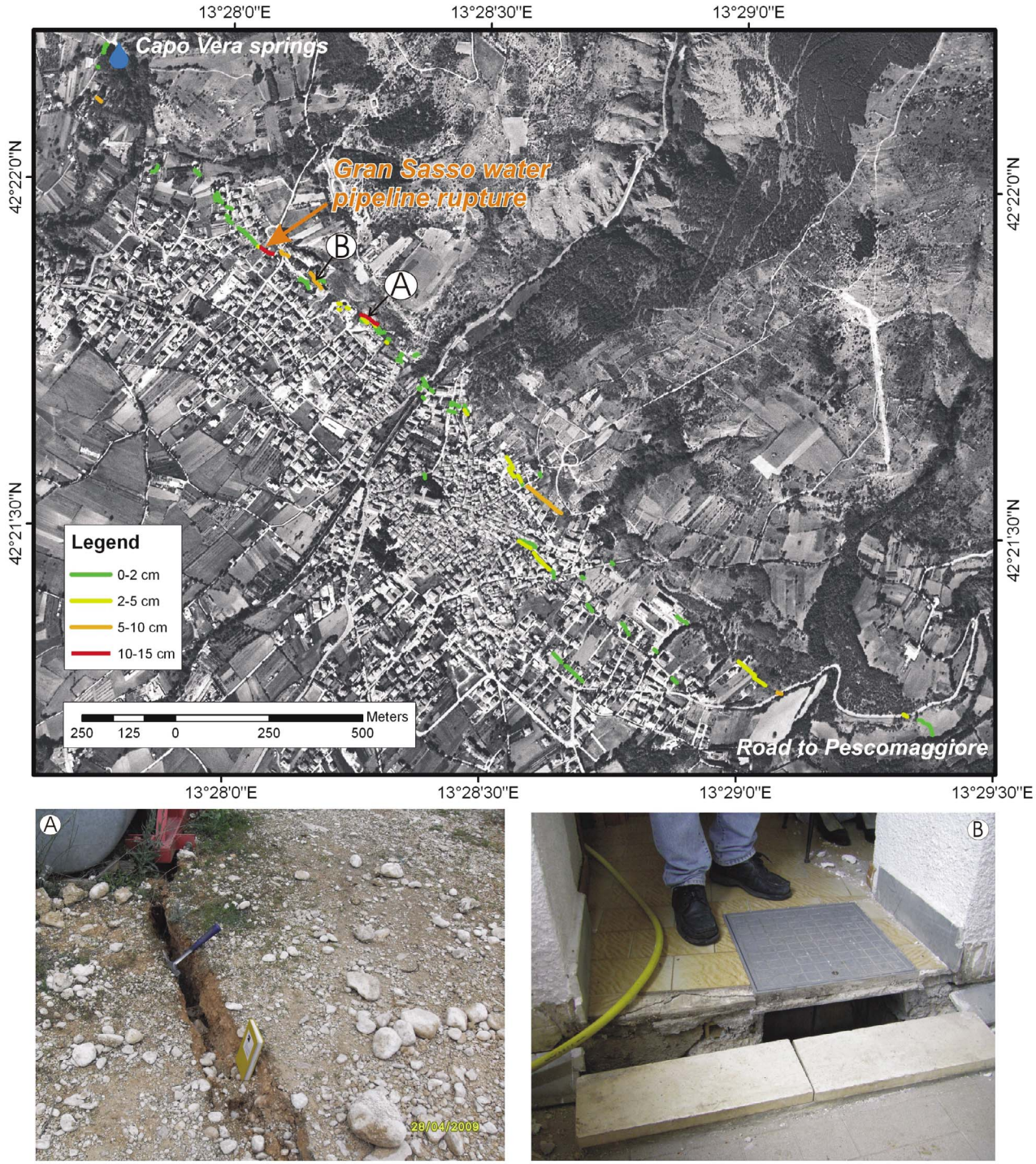

Figure 3. (top) Distribution of coseismic ground ruptures along the Paganica fault, colored according to the maximal measured vertical offsets (including postseismic offset). (bottom left and bottom right) Surface ruptures with offset in the ground (photograph A, more than 10 cm) and in buildings (photograph B, 7–8 cm).

satellite to ground line of sight (LOS) movement (Figure 4), and unwrapped interferograms that show the absolute displacement fields (Figure 5a). The general pattern of deformation is an oval-shaped subsidence southwest of the Paganica Fault reaching up to about 25 cm between the cities of L'Aquila and Fossa (center of fringes in Figure 4), and minor uplift of up to 5 cm northeast of the fault.

[26] Traces of surface ruptures are inferred from linear phase discontinuities identified in the interferogram (Figure 4). These phase changes suggest differential movements, and are thus interpreted as surface rupturing. The most prominent discontinuity (white line in Figure 4) corresponds to the surface faulting along the Paganica Fault. This lineament is about 12 km long, centered on the Paganica surface ruptures, and

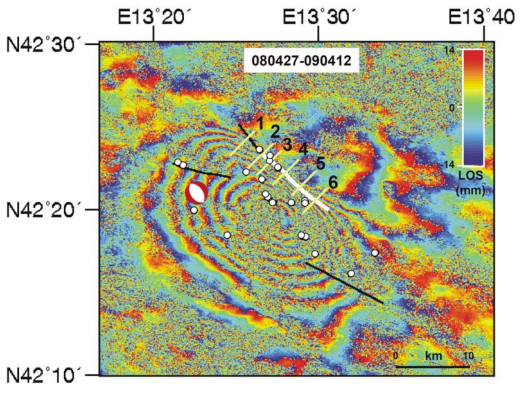

Figure 4. Wrapped descending interferogram showing fringe discontinuities that may be interpreted as fault ruptures (black lines). The Paganica fault rupture is marked by a white line. NE-SW trending yellow lines along this fault indicate the traces of LOS profiles (Figure 6). White dots indicate the field observations of coseismic ground ruptures in correspondence to mapped capable faults (see Figure 1 and Table 2). The location of the INGV-determined epicenter and its focal solution are also shown. A 90 m four-look interferogram of the same period is available in Figure S1.

extends both to the NW and to the SE. Three minor discontinuities (marked black) are seen at the northwestern extension of the Paganica Fault, and west and south of the fault (Figure 4).

[27] Displacement profiles across the Paganica Fault were made from the descending track interferogram (Figures 4 and 6) and are compared with ground truth values. Most profiles (numbers 1–5) show LOS displacements of up to 12 cm, decreasing to the NW and SE, in quite good agreement with the field observations (see discussion for a more detailed comparison).

3.3. Slip Distribution Along the Paganica Fault

[28] Previous models of the L'Aquila earthquake show ambiguous results regarding the upward extension of slip along the fault. *Walters et al.* [2009] show slip values of about 0.9 m at depth of about 9 km, gradually decreasing to 0.1 m at the surface, and *Papanikolaou et al.* [2010] showed that the InSAR predicted fault surface ruptures coinciding with localities where surface ruptures have been observed in the field, confirming that the ruptures observed near Paganica village are indeed primary. On the other hand, *Atzori et al.* [2009] concluded that the slip did not reach the surface, though some slip may have occurred at depths shallower than 1 km and locally reached very close to the surface.

[29] We invert the observed InSAR observations for fault parameters and slip distribution by a simple model based on solutions for dislocations in an elastic half-space [*Okada*, 1985]. We apply an inversion scheme [e.g., *Fialko*, 2004; *Hamiel and Fialko*, 2007] based on a least squares minimization of the displacement misfit with iterations for the fault geometry and including subsampling of the SAR data using a recursive quad-tree algorithm [e.g., *Jónsson et al.*, 2002]. The fault trace in our model was inferred from the main discontinuity in the interferogram (Figure 4). To account for nonplanar fault geometry and spatially variable slip, the fault surfaces were initially divided into two rectangular segments which were further subdivided into constant-slip patches, allowing only for normal slip mode. The size of these patches gradually increases from ~0.2 km (both along strike and downdip) at the top of the fault to ~3.5 km at the bottom of the fault, approximately in a geometric progression such that the model resolution is essentially independent of depth. In this way we could also detect in high resolution where exactly the surface rupture occurred, independently from the field evidence. Subsequently, we refined the fault plane geometry by allowing changes in the fault dip in order to minimize the data misfit in a nonlinear least squares inversion. The models were smoothed in order to minimize the slip gradients between the fault patches [e.g., *Fialko*, 2004] and positivity was imposed. The preferred slip model is selected on the basis of minimal RMS using the highest-possible smoothness.

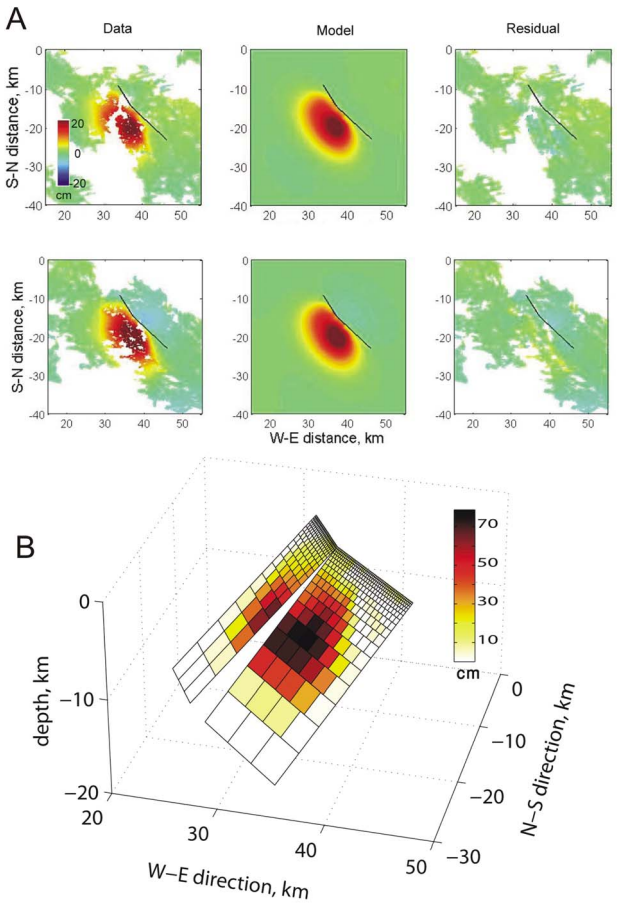

Figure 5. (a) Inversion of (top) ascending track 090311-090415 and (bottom) descending track 090201-090412 interferograms of the L'Aquila earthquake (local UTM coordinates, origin at 13°N, 42.5°S). (left) Original unwrapped interferograms. (middle) Model (synthetic) interferograms obtained by inversion of the corresponding data interferograms. (right) Residuals between interferograms and models. Positive values (red) mark movement away from the satellite. Fault traces, marked by black lines, follow fringe discontinuities in the interferograms and are extended to the NW and SE for the inversion. (b) Best fitted dip-slip model.

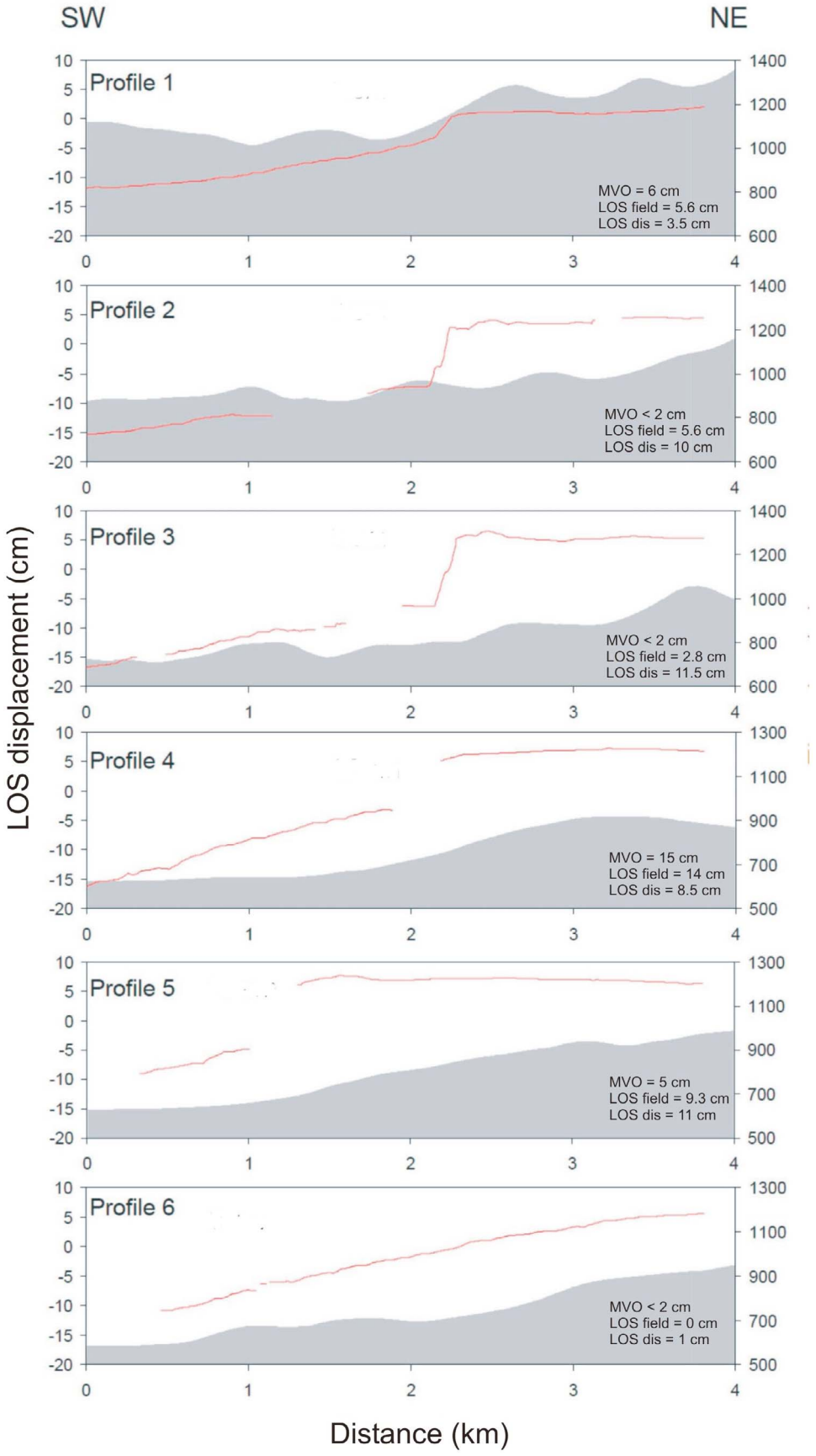
SW
NE
Profile 1
MVO = 6 cm
LOS field = 5.6 cm
LOS dis = 3.5 cm
Profile 2
MVO < 2 cm
LOS field = 5.6 cm
LOS dis = 10 cm
Profile 3
MVO < 2 cm
LOS field = 2.8 cm
LOS dis = 11.5 cm
Profile 4
MVO = 15 cm
LOS field = 14 cm
LOS dis = 8.5 cm
Profile 5
MVO = 5 cm
LOS field = 9.3 cm
LOS dis = 11 cm
Profile 6
MVO < 2 cm
LOS field = 0 cm
LOS dis = 1 cm
LOS displacement (cm)
Distance (km)

Figure 6

Table 1. Fault Parameters for the L'Aquila Earthquake From Previous Sources and the Current Study

Model[a]	Strike (deg)	Dip (deg)	Max Slip (m)	Length (km)	Top (km)	Bottom (km)	Moment by 1018 Nm
1	127	50					3.42
2	133	47	0.9	12.2	1.9	12.2	2.9
3	144	54	~0.9	19	0	13	2.91
4	133; 147[b]	45	0.8	18.5	0	11.7	2.88

[a]Model 1, Global Centroid Moment Tensor (GCMT) solution; model 2, *Atzori et al.* [2009]; model 3, *Walters et al.* [2009]; model 4, current study.
[b]Two segments.

[30] To assess the slip distribution on the Paganica rupture, we invert both the ascending and descending interferograms of the L'Aquila earthquake (Figure 5). The difference between the two interferograms is 3 days (12–15 April). A postseismic interferogram of 12 April to 17 May (Figure S2) shows very minor (if any) signal, thus we regard the postseismic signal during the 12–15 April interval as negligible compared to the coseismic signal. The coseismic signal also includes contributions from the main aftershocks until 15 April. We cannot reject the possibility that those events occurred along the main Paganica Fault, but we are unable to model the contribution of these events separately.

[31] Our best fit inverted model accounts for 96% of the observed deformation from both interferograms with an RMS value of 0.8 cm (Figure 5b).

[32] The model indicates coseismic dip-slip displacement during the L'Aquila earthquake on two fault segments dipping 45° to the southwest with maximum slip of about 80 cm at 7–9 km depth, below the village of Onna. The best fit source parameters obtained by our inversion is compared to previous studies in Table 1.

[33] The total calculated geodetic moment release is M0 = 2.88×10^{18} Nm (corresponding to a moment magnitude M_w 6.24), which is comparable to the geodetic moments calculated by previous InSAR studies of this earthquake and slightly smaller than the estimated moment derived from seismic data (Table 1). According to our model, slip occurred at the surface near the village of Paganica and three additional areas, one northwest and two southeast of Paganica. Each of these patches is a few hundred meters long. The maximum calculated slip near the surface is 15–20 cm. The overall calculated slip near the surface is consistent with field observations of up to 15 cm coseismic and postseismic vertical displacement in several areas, mostly at Paganica (e.g., Figure 6), allowing to confirm the primary nature of these ruptures (see also Figure 3).

4. Coseismic Ruptures Along Other Mapped Capable Faults

[34] In addition to the Paganica fault, several coseismic ruptures along other mapped capable faults were surveyed by us as well as by surveyors from other research institutes. These observations are shown in Figure 7 and summarized for each fault in Table 2 (Figure 1 for the location of observation points).

[35] Discontinuous and very local ground ruptures, some tens of meters long, with 15–20 cm offset, were found along the NW-SE trending Pettino Fault (north of L'Aquila). Along the Bazzano Fault, which is a normal fault antithetic to the Paganica Fault, a discontinuous free face (i.e., a narrow band at the base of limestone fault plane, often marked by brown soil, interpreted as an evidence of coseismic surface reactivation of normal faults) was observed for segments of some hundreds of meters with offsets locally up to 5–6 cm [see *Papanikolaou et al.*, 2010]. Fractures in the Ciuffino quarry and in the Bazzano industrial area are located along the NW and SE extension of the Caticchio Fault, a minor structure between the Paganica and Bazzano faults. Several fractures in paved roads (near Villa Sant'Angelo and Fossa villages) are consistent, in terms of trends and location, with the Monticchio-Fossa-Stiffe Fault. A free face about 1 cm wide and at least 1 km long was found along the 125°N trending Canetre fault not far from Roio. At Poggio di Roio, a fracture in paved road matches with this trend. Two fractures in cultivated fields and some other fractures and free faces mapped by *Messina et al.* [2009] have suggested the surface reactivation of the Valle degli Asini Fault, near the San Gregorio village. According to *Falcucci et al.* [2009] and *Boncio et al.* [2010], field evidences support the surface reactivation of about 1.3 km along the Colle Enzano fault segment, a normal structure located not far from Collebrincioni. Our surveys pointed out only some fractures with not relevant offsets located near Tempera and near Colle Enzano which match with the Colle Enzano fault segment. Moreover, *Galli et al.* [2009] found some ground ruptures in correspondence to the San Demetrio Fault.

[36] All the abovementioned effects are interpreted by us and/or by some other authors (see Table 2) as expressions of coseismic reactivation of other faults.

[37] In order to confirm this hypothesis we examined in detail the location of the minor linear phase discontinuities shown by the coseismic interferogram (Figure 4). The southern lineament is about 8 km long and is in quite good agreement with the Fossa and Stiffe fault segment. The northwestern lineament, about 3 km long, is quite consistent with the Colle Enzano fault, at the northwestern extension of the Paganica Fault. The western lineament is located west of San Giacomo and could be related to the Pettino fault. The three lineaments show offsets between less than half a fringe cycle and two cycles, are in places incoherent on one side and coincide with topographic relief of 600–800 m. A

Figure 6. Line of sight (LOS) displacements along six profiles (shown by red lines) crossing the Colle Enzano Fault (profiles 1 and 2) and the Paganica Fault (from profile 3 to profile 6). MVO, measured vertical offset on the field. LOS field, vertical offset projected on the satellite line of sight. LOS dis, radar line of sight displacement. Gray shaded areas show the corresponding topographic profiles. Trace of profiles are shown in Figure 4.

Figure 7. Details on surface ruptures along mapped capable faults (see Table 2 for description and Figure 1 for location).

close examination at the locations of the coseismic effects (Figures 3 and 4 and Table 2) shows no clear correspondence between surface effects and the southern lineament and good correlation with the western and northwestern linear discontinuities. A quantitative comparison between the amount of observed slip and fringe offsets (as shown in Figure 6 for the Paganica Fault) is hindered by the existence of incoherent strips at the margins of these phase discontinuities.

5. Discussion and Conclusions

[38] The scenario of surface ruptures triggered by the 2009 L'Aquila earthquake is typical for moderate ($6.0 < M < 6.5$) earthquakes in the Apennines, as clearly observed during similar events in the past 15 years [*Vittori et al.*, 2000; *Michetti et al.*, 2000]. Field observations documented unequivocally the pattern of surface faulting along the Paganica Fault, characterized by tectonic ruptures aligned for almost 3 km and vertical offsets frequently higher than 7–8 cm which increased to more than 10 cm in the postseismic phase [*Wilkinson et al.*, 2010]. These values are in agreement with a slip model derived from the inversion of InSAR measurements, which shows a maximum slip of ~80 cm at depth of 7–9 km decreasing to about 15 cm at the surface.

[39] At the NW extension of the Paganica Fault (Colle Enzano, Monte Castellano and Stabiata faults) the pattern of ruptures is more discontinuous and our surveys did not measure relevant displacements along these ruptures. Nonetheless, *Boncio et al.* [2010] measured vertical offsets up to 6 cm, where InSAR shows surface warping of up to 15 cm, confirming the occurrence of minor surface faulting even on the NW extension of the Paganica Fault.

[40] The SE extension of the Paganica Fault (e.g., the Valle degli Asini faults) is characterized by discontinuous ground cracks a few hundred meters long, with surface and LOS offsets that do not exceed 1 cm (Figure 6). Therefore, the hypothesized surface coseismic reactivation of this fault segment [*Galli et al.*, 2009] cannot be confirmed by field observations or by InSAR data.

Table 2. Coseismic Geological Effects That Occurred on Mapped Capable Faults (Field and InSAR Evidence)[a]

Fault Name	Description	Coseismic Effects	From Other Papers/Reports	Measured Field Offset	Observed InSAR Offset
Pettino	NW-SE trending SW dipping normal fault, about 3.5 km long, bordering the L'Aquila basin at NE, located at the base of a fault escarpment (about 350 m high) on the SW slope of Mt. Pettino. The fault has cut the tips of an Upper Pleistocene alluvial fan [*Servizio Geologico d'Italia*, 2006]. Paleoseismic investigations in the SE sector [*Galli et al.*, 2009] have shown that the fault displaces deposits of about 8 kyr (minimum age).	Open fractures, 280°N trending, a few meters long, and offset of about 5 cm marked by the upthrowing of leaves (**1**).	*Emergeo Working Group* [2010] describes ground ruptures along the Pettino fault, with offset up to 15–20 cm in soil and debris.	5 cm according to our surveys and 15–20 cm according to *Emergeo Working Group* [2010].	No appreciable LOS offset
Bazzano	NW-SE trending NE dipping normal fault, about 3 km long, at the base of the NE slope of Mt. Bazzano carbonate ridge. An evident fault escarpment is associated to this fault. Alluvial fan deposits (Middle Pleistocene) in the hanging wall are covered by recent colluvial deposits and, locally, by travertines.	A free face (brown stripe at the base of a white band) 2 cm high and up to 30 m long was observed (**2**). Ground cracks were observed in the asphalt road to Bazzano village, probably associated with coseismic slope movement (**3**). A 75°N trending fracture, 7 m long and a few millimeters wide located in the hanging wall of the northern segment of the Bazzano fault, was observed across an asphalt road (**4**).	*Falcucci et al.* [2009] describe a free face up to 15 cm high, a few meters long, at the base of the fault plane, at the NW end of the fault, probably mainly due to non-tectonic gravitational processes and/or compaction. Nevertheless, they cannot exclude a tectonic component. *Emergeo Working Group* [2010] documented a whitish fault ribbon with a constant height of about 5 cm at the base of bedrock fault plane, and other discontinuous scarps in unconsolidated slope deposits for about 1 km, suggesting vertical displacements of 0.1–0.3 m.	2 cm according to our surveys and 5 cm according to *Emergeo Working Group* [2010].	No appreciable LOS offset
Caticchio	NW-SE trending, NE dipping normal fault, about 2 km long, at the NE slope of Monte Caticchio. Alluvial deposits crop out in the hanging wall. A new fault escarpment is not evident. At the NW end of the fault, in the Ciuffino quarry, it cuts Quaternary deposits (**5**).	A system of eight main fractures (**5**) were mapped in the Ciuffino quarry (strike, between 90°N and 100°N; width, some millimeters; length, 4–5 m). A survey repeated a few days later showed the progressive growth of one fracture and the appearance of two additional fractures, subparallel to the previous ones. Some other fractures (**6**) were mapped at the NW border of the Bazzano industrial area (strike, 160°N–		<1 cm	No appreciable LOS offset

Table 2. (continued)

Fault Name	Description	Coseismic Effects	From Other Papers/Reports	Measured Field Offset	Observed InSAR Offset
		170°N; width, 3–5 cm; length, about 20–30 m). This system, although not located in correspondence to mapped faults, is in good agreement with the trend of the Monte Caticchio normal fault.			
Monticchio-Fossa-Stiffe	The NW-SE trending NE dipping Monticchio-Fossa-Stiffe normal fault is located at the base of the eastern slope of the Monti d'Ocre carbonate relief, from Monticchio to SE of Stiffe. It is composed of three main fault segments: (1) the Monticchio fault segment (strike 330°N) about 3.5 km long; (2) the Fossa fault segment (strike 310°N) about 2.5 km long; and (3) the Stiffe fault segment (strike 310°N) about 7.5 km long. Mesozoic carbonate rocks crop out in the footwall and Quaternary alluvial deposits covered by slope deposits characterize the hanging wall.	Near Villa Sant Angelo, fractures (strike, 130°N; width, some centimeters; length >30 m) affecting paved roads are located in correspondence with the Fossa fault segment. Nevertheless, the fractures appear to be more likely linked to the failure of a retaining wall parallel to the road, induced by gravitative phenomena (**7**). NW of Fossa, a set of five parallel fractures (strike, 120°N–130°N. Width, 1–2 cm; length, <2 m; 8–10 m apart) have affected the paved road. The most deformed zone showed evidence of compression (**8**). About 200 m from the previous site, mud volcanoes were mapped by *Emergeo Working Group* [2010]. One fracture up to 1 cm wide and about 100 m long was observed on an asphalt road SE of Fossa, parallel to the trend of the Fossa Fault (**9**).	In the footwall of the Monticchio fault segment, *Emergeo Working Group* [2010] highlighted the presence of an open fracture on the top of the scarp. The fracture appears compatible with the reactivation of an associated minor fault or a conjugate set of fractures. Near the Fossa village, surface ruptures at least 300 m long were found close to the recent geomorphic scarps.	<1 cm	All the measured field points are in decorrelated areas so it is impossible to measure LOS.
Roio-Canetre	The NW-SE trending, SW dipping Roio-Canetre normal fault is located on the SW slope of the carbonate ridge developed from Poggio of Roio to Bagno. The fault is made by two major segments about 4 and 1 km long. The fault cuts Mesozoic carbonate rocks in the footwall and partially in hanging wall where they are associated with Quaternary breccias and colluvial deposits.	A free face (brown stripe at the base of a white band) 1 cm high and about 1 km long was observed at the SE termination of the NW fault segment, affecting rock debris and rock-to-rock contacts. This could support a primary origin for this feature (**10**). At Poggio di Roio, a coseismic fracture crossed an asphalt road and a concrete wall (**11**). The location and the geometry of the	*Emergeo Working Group* [2010] describes a fresh free face scarp with a constant height up to 30 mm associated with local fissuring, for a minimum length of 1 km. A 5–10 cm white stripe at the base of the Roio fault scarp is reported by *Boncio et al.* [2010].	about 1 cm	No appreciable LOS offset

Table 2. (continued)

Fault Name	Description	Coseismic Effects	From Other Papers/Reports	Measured Field Offset	Observed InSAR Offset
	Several karst depressions (the so-called *Canetre*) are distributed along the fault.	fracture (about 80 m long, strike 100°N, vertical offset about 4 cm toward south, width 1 cm) is in good agreement with the fault geometry. Nevertheless it could be related to the collapse of the road embankment.			
Valle degli Asini	NW-SE trending normal fault, about 2 km long, bordering the Valle degli Asini up to San Gregorio. The fault shows en echelon geometry with the Paganica fault. It cuts carbonate rocks and Late Pleistocene–Holocene alluvial deposits.	Two fractures (**12**) were found in farmed fields (strike, 130°N; width, 2–3 cm; length, at least 70–80 m. According to local eyewitnesses, the second one continued up to the top of the hill.	*Messina et al.* [2009] point out diverse evidence of surface faulting (fractures and free faces) SE of San Gregorio village and along the trend of the fault. *Boncio et al.* [2010] refer to another alignment of coseismic ground fractures, about 4 km long, between San Gregorio and the Bazzano industrial area. According to the authors it consists of a set of discontinuous en echelon metric fissures, up to few centimeters wide, with no vertical throw, directed WNW-ESE at San Gregorio and NW-SE further to southeast. These fractures are correlated by the authors to a WNW-ESE directed, SW dipping fault buried below Pleistocene fan deposits, found by geophysical investigations.	<1 cm	No appreciable LOS offset
San Demetrio	The San Demetrio fault is made by three NW-SE trending parallel en echelon fault segments, 2 to 4 km long. It displaces Middle Pleistocene alluvial fan deposits.	Very thin coseismic ground cracks were observed in a paved road at La Villa Grande village (**13**), both at the base and at the top of the fault scarp associated with the central fault.	*Galli et al.* [2009] describe ground ruptures in the field, along the roads and on buildings within the San Demetrio ne' Vestini village, in correspondence to the San Demetrio fault plane and its hanging wall.	<1 cm	No appreciable LOS offset
Colle Enzano	A NW-SE trending (strike 325°N) SW dipping normal fault runs from San Biagio to Colle Enzano for about 2.5 km, showing an en echelon geometry with the Paganica fault. According to *Servizio Geologico d'Italia* [2006], it is about 1 km long, affects Mesozoic carbonate rocks, without evidence of Quaternary activity.	Thin ground cracks (**16**) a few meters long were seen on a dirt road to the east of Colle Cocurello and on the Aragno–San Giacomo road. Near San Biagio, not far from Tempera, one small fracture (strike 50°N) affected a dirt road (**14**) in correspondence with the fault. A set of fractures (strike about 135°N) was observed at the	According to *Falcucci et al.* [2009] discontinuous evidence of reactivation of the Colle Enzano fault was observed from San Biagio to about 1.5 km SE of Collebrincioni where along the northern part of the fault segment a fresh-looking free face up to 8–10 cm high was recognized (**17**). According to *Boncio et al.* [2010] the	<1 cm according to our surveys; 4–6 cm according to *Boncio et al.* [2010]	The measured field point shows 35 mm offset in LOS, which, assuming that all the displacement is vertical, corresponds to about 40 mm vertical displacement.

Table 2. (continued)

Fault Name	Description	Coseismic Effects	From Other Papers/Reports	Measured Field Offset	Observed InSAR Offset
		intersection between the fault and the viaduct Vigne Basse of the A24 highway. Among them, the major fracture was about 5 mm wide and about 4 m long, while the other cracks were very thin and less than 1 m long (**15**).	reactivation of the Colle Enzano segment is indicated by a continuous coseismic free face (**17**) at the base of the preexisting fault scarp with maximum throw up to 4–6 cm and apertures of 4 to 8 cm in the northern part of the fault and fractures with offset up to 2–3 cm in the southern part (**18**).		
Monte Castellano	A NW-SE trending SW dipping normal fault running at the base of the Mt. Castellano ridge for about 1.7 km. The fault represents the northern segment of the Paganica–San Demetrio fault system. The fault is characterized by a continuous fault scarp carved in limestone rocks at the footwall and by late Quaternary debris at the hanging wall.		According to *Boncio et al.* [2010] free faces 2 to 6 cm high were mapped at the base of the fault scarp and hanging wall right-stepping fractures on late Quaternary debris were observed a few meters from the fault trace (19).	2–6 cm according to *Boncio et al.* [2010]	About 3.5 cm of LOS offset
Monte Stabiata	An arcuate shape SSW dipping about 4 km long normal fault running along the SW flank of Mt. Stabiata. The western sector of the fault strikes E-W, whereas the eastern sector strikes NW-SE. The fault is characterized by a prominent escarpment carved in limestone rocks at the footwall and by late Quaternary debris at the hanging wall.		According to *Boncio et al.* [2010] coseismic effects were recognized along the southern end of the NW-SE trending segment of the fault where a free face 3 to 6 cm high and fractures were observed (20).	3–6 cm according to *Boncio et al.* [2010]	InSAR does not show a surface break at this point but it shows a clear flexure which means that there is probably a fault at the near subsurface.

[a]Locations are mapped in Figure 1. Surface effects along the Paganica Fault are shown in Figure 3. Fault abbreviations are as follows: Pettino, PET; Bazzano, BAZ; Caticchio, CAT; Monticchio-Fossa-Stiffe, MFS; Roio-Canetre, ROC; Valle degli Asini, VAS; San Demetrio, SDE; Colle Enzano, CEN; Monte Castellano, MCS; Monte Stabiata, STB. Bold numbers refer to the sites mapped in Figure 1.

[41] The same approach was applied to other mapped capable faults. Along the Monticchio-Fossa-Stiffe Fault field and InSAR evidence seem to be in good agreement, however, the InSAR results are contaminated by topographic contribution and decorrelated on one side of the fault, and are thus somewhat questionable.

[42] Along some other faults (e.g., the Pettino and Bazzano faults) offsets were locally comparable to the maximum offsets of the Paganica ground ruptures: however, these features were very discontinuous and appear to be more likely induced by the shaking. The InSAR evidence along the Pettino Fault may indicate reactivation, but cannot be used as a direct evidence of surface faulting, since they are decorrelated on one side and are not supported by robust field evidence.

[43] Along the Roio-Canetre fault, a fresh free face in rock, 1 cm high and more than 1 km long, associated with rock debris and rock-to-rock tectonic contacts suggested a primary origin. Such minor deformation cannot be seen in by InSAR.

[44] In conclusion, this study has demonstrated that the combination of field observations and InSAR measurements prove to be very helpful for detecting continuous surface ruptures, even for moderate events such as the L'Aquila earthquake. Our study shows unequivocally that the Paganica Fault did generate coseismic surface faulting, for a minimum rupture length of ~3 km. The consistency between field and InSAR observation allows to confirm that the Paganica Fault is the causative tectonic structure for the L'Aquila event, and that the tectonic rupture along this structure propagated from ~9 km directly to the ground surface.

[45] However, our study also shows that several limitations still exist even for an exceptionally well documented case history such as the one analyzed in this paper. When surface ruptures are short, discontinuous and show small displacements (typically smaller than 1–2 cm), the combined approach may be less helpful due to resolution boundaries. In such cases, the genetic interpretation of the ground rupture mechanisms may not always be clear.

[46] Nevertheless, remote sensing, and particularly InSAR, is expected to play an important role in future support of field surveys, thanks to the new constellations of dedicated satellites (e.g., Sentinel-1 by ESA) which will significantly improve the frequency of coverage and resolution of imaging after destructive earthquakes, which still are the major drawbacks of satellite potential contribution to hazard and disaster assessment (e.g., GMES program and the GEO initiative).

6. Data Source

[47] Data sources for seismological data are as follows: EMSC, http://www.emsc-csem.org/; INGV, http://iside.rm.ingv.it; USGS, http://earthquake.usgs.gov/regional/neic/. Data source for historical seismic catalog is as follows: CPTI08, http://emidius.mi.ingv.it/CPTI08. Data source for capable faults is as follows: ITHACA, Italian Hazard from Capable faults, http://193.206.192.227/wms_dir/Catalogo_delle_Faglie_Capaci_ITHACA.html. The other data used in this paper came from published sources listed in the references.

[48] **Acknowledgments.** This research benefited from invaluable discussion on the L'Aquila earthquake ruptures with Gerald Roberts and Leonello Serva. Funding to G.S. has been provided by a University of Insubria urgent grant. ENVISAT ASAR images were provided by the European Space Agency under project C1P.5544.

References

Atzori, S., I. Hunstad, M. Chini, S. Salvi, C. Tolomei, C. Bignami, S. Stramondo, E. Transatti, A. Antonioli, and E. Boschi (2009), Finite fault inversion of DInSAR coseismic displacement of the 2009 L'Aquila earthquake (central Italy), *Geophys. Res. Lett.*, *36*, L15305, doi:10.1029/2009GL039293.

Azzaroli, A. (1977), The Villafranchian stage in Italy and the Plio-Pleistocene boundary, *G. Geol.*, *41*(2), 61–79.

Baer, G., Y. Hamiel, G. Shamir, and R. Nof (2008), Evolution of a magma-driven earthquake swarm and triggering of the nearby Oldoinyo Lengai eruption, as resolved by InSAR, ground observations and elastic modeling, East African Rift, 2007, *Earth Planet. Sci. Lett.*, *272*, 339–352, doi:10.1016/j.epsl.2008.04.052.

Bagnaia, R., A. D'Epifanio, and S. Sylos Labini (1992), Aquila and subaequan basins: An example of Quaternary evolution in central Apennines, Italy, *Quat. Nova, II*, 187–209.

Baratta, M. (1901), *I Terremoti d'Italia: Saggio di Storia, Geografia e Bibliografia Sismica Italiana*, Fratelli Bocca, Vigevano, Italy.

Biggs, J., E. Bergman, B. Emmerson, G. J. Funning, J. Jackson, B. Parsons, and T. J. Wright (2006), Fault identification for buried strike-slip earthquakes using InSAR: The 1994 and 2004 Al Hoceima, Morocco earthquakes, *Geophys. J. Int.*, *166*, 1347–1362, doi:10.1111/j.1365-246X.2006.03071.x.

Blumetti, A. M. (1995), Neotectonic investigations and evidence of paleoseismicity in the epicentral area of the January–February 1703 central Italy earthquakes, *Bull. Assoc. Eng. Geol.*, *6*, 83–100.

Blumetti, A. M., and L. Guerrieri (2007), Fault-generated mountain fronts and the identification of fault segments: Implications for seismic hazard assessment, *Boll. Soc. Geol. Ital.*, *126*(2), 307–321.

Blumetti, A. M., L. Guerrieri, F. Dramis, B. Gentili, A. M. Michetti, and E. Tondi (2004), P65—Basin and range in central Apennines, in *32nd IGC: Field Trip Guidebooks*, *Mem. Descr. Carta Geol. Ital.*, *63*(6), 1–48.

Blumetti, A. M., V. Comerci, P. Di Manna, L. Guerrieri, and E. Vittori (2009), Geological effects induced by the L'Aquila earthquake (6 April 2009, M_l = 5.8) in the natural environment, report, 38 pp., Ist. Super. per la Prot. e la Ric. Ambientale, Rome. (Available at http://www.apat.gov.it/site/en-GB/Projects/INQUA_Scale/Documents/.)

Boncio, P., A. Pizzi, F. Brozzetti, G. Pomposo, G. Lavecchia, D. Di Naccio, and F. Ferrarini (2010), Coseismic ground deformation of the 6 April 2009 L'Aquila earthquake (central Italy, M_w6.3), *Geophys. Res. Lett.*, *37*, L06308, doi:10.1029/2010GL042807.

Chiarabba, C., et al. (2009), The 2009 L'Aquila (central Italy) M_w6.3 earthquake: Main shock and aftershocks, *Geophys. Res. Lett.*, *36*, L18308, doi:10.1029/2009GL039627.

D'Agostino, N., R. Giuliani, M. Mattone, and L. Bonci (2001), Active crustal extension in the central Apennines (Italy) inferred from GPS measurements in the interval 1994–1999, *Geophys. Res. Lett.*, *28*, 2121–2124, doi:10.1029/2000GL012462.

D'Agostino, N., A. Avallone, D. Cheloni, E. D'Anastasio, S. Mantenuto, and G. Selvaggi (2008), Active tectonics of the Adriatic region from GPS and earthquake slip vectors, *J. Geophys. Res.*, *113*, B12413, doi:10.1029/2008JB005860.

Demangeot, J. (1965), *Geomorpholgiè des Abruzzes Adriatiques: Memoirs et Documents*, 403 pp., Ed. du Cent. Natl. de la Rech. Sci., Paris.

Emergeo Working Group (2010), Evidence for surface rupture associated with the M_w 6.3 L'Aquila earthquake sequence of April 2009 (central Italy), *Terra Nova*, *22*, 43–51, doi:10.1111/j.1365-3121.2009.00915.x.

Falcucci, E., et al. (2009), The Paganica Fault and surface coseismic ruptures caused by the 6 April 2009 earthquake (L'Aquila, central Italy), *Seismol. Res. Lett.*, *80*, 940–950, doi:10.1785/gssrl.80.6.940.

Fialko, Y. (2004), Probing the mechanical properties of seismically active crust with space geodesy: Study of the coseismic deformation due to the 1992 M_w 7.3 Landers (southern California) earthquake, *J. Geophys. Res.*, *109*, B03307, doi:10.1029/2003JB002756.

Galadini, F., and P. Galli (2000), Active tectonics in the central Apennines (Italy)—Input data for seismic hazard assessment, *Nat. Hazards*, *22*, 225–268, doi:10.1023/A:1008149531980.

Galli, P., R. Camassi, R. Azzaro, F. Bernardini, S. Castenetto, D. Molin, E. Peronace, A. Rossi, M. Vecchi, and A. Tertulliani (2009), Il terremoto aquilano del 6 Aprile 2009: Rilievo macrosismico, effetti di superficie ed implicazioni sismotettoniche, *Quaternario*, *22*, 235–246.

Goldstein, R. M., and C. L. Werner (1998), Radar interferogram filtering for geophysical applications, *Geophys. Res. Lett.*, *25*, 4035–4038, doi:10.1029/1998GL900033.

Goldstein, R. M., H. A. Zebker, and C. L. Werner (1988), Satellite radar interferometry: Two-dimensional phase unwrapping, *Radio Sci.*, *23*, 713–720, doi:10.1029/RS023i004p00713.

Hamiel, Y., and Y. Fialko (2007), Structure and mechanical properties of faults in the North Anatolian Fault system from InSAR observations of coseismic deformation due to the 1999 Izmit (Turkey) earthquake, *J. Geophys. Res.*, *112*, B07412, doi:10.1029/2006JB004777.

Jónsson, S., H. Zebker, P. Segall, and F. Amelung (2002), Fault slip distribution of the 1999 M_w 7.1 Hector Mine earthquake, California, estimated from satellite radar and GPS measurements, *Bull. Seismol. Soc. Am.*, *92*, 1377–1389, doi:10.1785/0120000922.

Maccagno, A. M. (1962), *L'Elephas Meridionalis, NESTI di Contrada "Madonna della Strada," Scoppito (L'Aquila)*, Stab. Tipograf. G. Genovese, Naples, Italy.

Massonnet, D., and K. L. Feigl (1998), Radar interferometry and its applications to changes in the Earth's surface, *Rev. Geophys.*, *36*, 441–500, doi:10.1029/97RG03139.

McCaffrey, K. J., et al. (2009), Post-seismic slip on the 6th April 2009 L'Aquila earthquake surface rupture, measured using a terrestrial laser scanner (tripod-mounted lidar), *Eos Trans. AGU*, *90*(52), Fall Meet. Suppl., Abstract U23A-0023.

Messina, A. P., P. Galli, B. Giaccio, and E. Peronace (2009), Quaternary tectonic evolution of the area affected by the Paganica fault (2009 L'Aquila earthquake), paper presented at 28th GNGTS National Conference, Osserv. Geofis. Sper., Trieste, Italy.

Michetti, A. M., F. Brunamonte, L. Serva, and E. Vittori (1996), Trench investigations along the 1915 Fucino earthquake fault scarps (Abruzzo, central Italy): Geological evidence of large historical events, *J. Geophys. Res.*, *101*, 5921–5936, doi:10.1029/95JB02852.

Michetti, A. M., L. Ferreli, E. Esposito, S. Porfido, A. M. Blumetti, E. Vittori, L. Serva, and G. P. Roberts (2000), Ground effects during the September 9, 1998, M_w = 5.6, Lauria earthquake and the seismic potential of the aseismic Pollino region in southern Italy, *Seismol. Res. Lett.*, *71*, 31–46.

Moro, M., V. Bosi, F. Galadini, P. Galli, B. Giaccio, P. Messina, and A. Sposato (2002), Analisi paleosismologiche lungo la faglia del M. Marine (alta valle dell'Aterno): Risultati preliminari, *Quaternario*, *15*, 267–278.

Okada, Y. (1985), Surface deformation due to shear and tensile faults in a half space, *Bull. Seismol. Soc. Am.*, *75*, 1135–1154.

Papanikolaou, I. D., G. P. Roberts, and A. M. Michetti (2005), Fault scarps and deformation rates in Lazio-Abruzzo, central Italy: Comparison between geological fault slip-rate and GPS data, *Tectonophysics*, *408*(1–4), 147–176.

Papanikolaou, I. D., M. Foumelis, I. Parcharidis, E. L. Lekkas, and I. G. Fountoulis (2010), Deformation pattern of the 6 and 7 April 2009, M_w = 6.3 and M_w = 5.6 earthquakes in L'Aquila (central Italy) revealed by ground and space observations, *Nat. Hazards Earth Syst. Sci.*, *10*, 73–87, doi:10.5194/nhess-10-73-2010.

Parozzani, G. (1887), *Notizie Intorno al Terremoto del 2 Febbraio 1703 Ricavate dai Manoscritti Antinoriani*, Tip. B. Vecchioni, L'Aquila, Italy.

Patacca, E., P. Scandone, M. Bellatalla, N. Perilli, and U. Santini (1992), La zona di giunzione tra l'arco appenninico settentrionale e l'arco appenninico meridionale nell'Abruzzo e nel Molise, *Studi Geol. Camerti*, *1991/2*, 417–441.

Price, E. J., and D. T. Sandwell (1998), Small-scale deformation associated with the 1992 Landers, California, earthquake mapped by synthetic aperture radar interferometry phase gradient, *J. Geophys. Res.*, *103*, 27,001–27,016, doi:10.1029/98JB01821.

Roberts, G. P., et al. (2010), Shallow subsurface structure of the 2009 April 6 M_w 6.3 L'Aquila earthquake surface rupture at Paganica, investigated with ground-penetrating radar, *Geophys. J. Int.*, *183*, 774–790, doi:10.1111/j.1365-246X.2010.04713.x.

Rosen, P. A., S. Henley, G. Peltzer, and M. Simons (2004), Updated repeat orbit interferometry package released, *Eos Trans. AGU*, *85*(5), 35, doi:10.1029/2004EO050004.

Salvi, S., et al. (2000), Modeling coseismic displacements resulting from SAR interferometry and GPS measurements during the Umbria-Marche seismic sequence, *J. Seismol.*, *4*, 479–499, doi:10.1023/A:1026502803579.

Serva, L., A. M. Blumetti, L. Guerrieri, and A. M. Michetti (2002), The Apennine intermountain basins: The result of repeated strong earthquakes over a geological time interval, *Boll. Soc. Geol. Ital.*, *1*, 939–946.

Servizio Geologico d'Italia (2006), Carta geologica d'Italia alla scala I:50.000, sheet 359, APAT, Rome, Italy.

Uria de Llanos, A. (1703), *Relazione o Vero Itinerario Fatto dall'Auditore Alfonso Uria de Llanos per Riconoscere li Danni Causati dalli Passati Terremoti Seguiti li 14 Gennaro e 2 Febbraro MDCCIII*, Stamperia Gaetano Zenobi, Rome.

Valensise, G. (2009), Faglie attive e terremoti: Tempo di cambiare strategie, *Geoitalia*, *28*, 12–17.

Vezzani, L., and F. Ghisetti (1998), Carta geologica dell'Abruzzo, scale 1:100,000, Soc. Elaborazioni Cartogr., Florence, Italy.

Vittori, E., et al. (2000), Ground effects and surface faulting in the September–October 1997 Umbria-Marche (central Italy) seismic sequence, *J. Geodyn.*, *29*, 535–564, doi:10.1016/S0264-3707(99)00056-3.

Walters, R. J., J. R. Elliott, N. D'Agostino, P. C. England, I. Hunstad, J. A. Jackson, B. Parsons, R. J. Phillips, and G. Roberts (2009), The 2009 L'Aquila earthquake (central Italy): A source mechanism and implications for seismic hazard, *Geophys. Res. Lett.*, *36*, L17312, doi:10.1029/2009GL039337.

Wilkinson, M., et al. (2010), Partitioned postseismic deformation associated with the 2009 M_w 6.3 L'Aquila earthquake surface rupture measured using a terrestrial laser scanner, *Geophys. Res. Lett.*, *37*, L10309, doi:10.1029/2010GL043099.

R. Amit, G. Baer, Y. Hamiel, A. Mushkin, and A. Salamon, Geological Survey of Israel, 30 Malkhe Yisrael St., Jerusalem 95501, Israel.

A. M. Blumetti, V. Comerci, P. Di Manna, L. Guerrieri, and E. Vittori, Geological Survey of Italy, High Institute for the Environmental Protection and Research, Via Brancati 48, I-00144 Roma, Italy. (luca.guerrieri@isprambiente.it)

A. M. Michetti and G. Sileo, Dipartimento di Scienze Chimiche ed Ambientali, Facoltà di Scienze Matematiche, Fisiche e Naturali, Università degli Studi dell'Insubria, Via Valleggio 11, I-22100 Como, Italy.